

CrystEngComm

Accepted Manuscript



This is an *Accepted Manuscript*, which has been through the Royal Society of Chemistry peer review process and has been accepted for publication.

Accepted Manuscripts are published online shortly after acceptance, before technical editing, formatting and proof reading. Using this free service, authors can make their results available to the community, in citable form, before we publish the edited article. We will replace this *Accepted Manuscript* with the edited and formatted *Advance Article* as soon as it is available.

You can find more information about *Accepted Manuscripts* in the [Information for Authors](#).

Please note that technical editing may introduce minor changes to the text and/or graphics, which may alter content. The journal's standard [Terms & Conditions](#) and the [Ethical guidelines](#) still apply. In no event shall the Royal Society of Chemistry be held responsible for any errors or omissions in this *Accepted Manuscript* or any consequences arising from the use of any information it contains.

Fast crystallization and low-power amorphization of Mg-Sb-Te reversible phase-change films

Junjian Li^a, Guoxiang Wang^b, Jun Li^a, Xiang Shen,^{b†} Yimin Chen^a, Rongping Wang^c, Tiefeng Xu^{a,b}, Qiuhua Nie^{a,b}, Shixun Dai^b, Yegang Lu^a, Xunsi Wang^b

We prepared Mg-doped Sb₂Te films and investigated their structural, optical and electric properties. It was found that, Mg-doping can increase the crystallization temperature, suppress the crystal growth and shorten crystallization time of Sb₂Te. Compared with Ge₂Sb₂Te₅, the optimal composition Mg_{21.5}(Sb₂Te)_{78.5} exhibits a higher crystallization temperature (~183 °C), larger crystallization activation energy (~3.86 eV) and better data retention ability (keeping the amorphous state at ~121 °C for ten years), indicating improved amorphous state stability due to the formation of Mg-Sb bonds. A reversible repetitive optical switching behavior was realized in the Mg_{21.5}(Sb₂Te)_{78.5} film with a fast crystallization speed of 52 ns and a low amorphization power of 35 mW.

The search for high performance phase change material is motivated by the development of phase change memory (PCM) technology with good thermal stability and crystallization speed. Generally, the development of high-density memory arrays requires the phase change material with higher stability of the amorphous phase to boost data retention and higher crystalline resistance to lower RESET current.¹ Unfortunately, no generic materials can meet these criteria. For example, Ge₂Sb₂Te₅ is a phase change material that has been widely investigated and regarded as the best one. However, several issues, including low crystallization temperature (~168°C), slow crystallization speed and low crystalline resistance have led to poor data retention, long programming time and large RESET current in the PCM device.² Therefore it is necessary to further optimize the material properties. One of the strategies is to add the impurities into phase change material to improve the physical performance of PCM. It has been reported that, doping of foreign elements such as Zn,³ Al,⁴ Cu,⁵ and Ti⁶ can improve the data retention and power consumption of PCM devices.

In order to enhance the thermal stability and crystalline resistance as well as maintain the fast crystallization speed, suitable phase change hosts and impurities appears to be important. Among various materials alternative, Sb-Te alloy has a fast crystallization speed due to its growth-dominated crystallization mechanism. However, pure Sb-Te has a low crystallization temperature (~100°C), a high melting temperature (~616°C) and a low crystalline resistance, leading to poor data retention and high power consumption of PCM.⁷ On the other hand, our previous work⁸ indicated that Mg doping could enhance the performance of Ge₂Sb₂Te₅ effectively. Therefore, in this paper, Mg-doped Sb₂Te films were prepared and their phase change properties were systematically studied in order to explore the best material with a high thermal stability and a fast crystallization speed. Through various experimental methods including the measurements of sheet resistance versus temperature (R-T), X-ray diffraction (XRD) patterns, and X-ray photoelectron spectra (XPS), the effect of Mg doping on crystallization characteristics, thermal stability, and electrical resistance of the Sb₂Te films was analyzed. The crystallization temperature within an acceptable range was tuned, and the reliability of this microstructure during repetitive laser melt-quenching cycles was tested.

Mg_x(Sb₂Te)_{1-x} thin films with a thickness of ~200 nm were deposited on Si and SiO₂ wafers at room temperature by magnetron co-sputtering using separated Mg and Sb₂Te targets. The chamber pressure was evacuated to 2×10⁻⁴ Pa, and then Ar gas was introduced to 3.5 Pa during the sputtering. The compositions of the Mg_x(Sb₂Te)_{1-x} films were determined by means of energy dispersive spectroscopy (EDS) with an error less than 0.5 at%. Moreover, we found that thermal annealing has negligible effect on film compositions. Temperature-dependent resistance measurements were *in situ* performed in a vacuum chamber at a heating rate of

[†] Corresponding authors at: Laboratory of Infrared Material and Devices, Advanced Technology Research Institute, Ningbo University; Ningbo 315211, China Tel.: 0574-87600947; fax: 0574-97600946; e-mail: shenxiang@nbu.edu.cn

40 K/min. The change of time-dependent resistance at isothermal annealing temperatures was also utilized to characterize the data retention of the amorphous films. X-ray diffraction (XRD) in the 2θ range of $20\sim 60^\circ$ using $\text{Cu K}\alpha$ radiation was employed to characterize the crystalline structure of films. The surface morphology was examined by atomic force microscopy (AFM). X-ray photoelectron spectroscopy (XPS) was used to probe the chemical bonding states of the elements. A static laser tester (PST-1, NANOSStorage Co. Ltd., KOREA) with a wavelength of 658nm was used to characterize crystallization behavior and optical switching test. The change of the laser power was from 5mW to 70mW, and that of the pulse width was from 5 to 250ns.

Figs. 1(a) and (b) show the sheet resistance as a function of temperature (R-T) for Mg-doped Sb_2Te films at a heating rate of 40K/min. The sheet resistance of the as-deposited film increases with increasing Mg content at room temperature, but decreases slowly with increasing temperature up to their respective crystallization temperature (T_c) which is determined by the minimum of the derivative of *in situ* R-T curve.⁹ T_c value of the $\text{Mg}_{6.1}(\text{Sb}_2\text{Te})_{93.9}$, $\text{Mg}_{9.5}(\text{Sb}_2\text{Te})_{90.5}$, $\text{Mg}_{13.1}(\text{Sb}_2\text{Te})_{86.9}$, $\text{Mg}_{21.5}(\text{Sb}_2\text{Te})_{78.5}$ films is ~ 161 , ~ 173 , ~ 178 and $\sim 183^\circ\text{C}$, respectively, all of which are higher than T_c of Sb_2Te ($\sim 144^\circ\text{C}$). It indicates that, increasing Mg content can effectively raise T_c of the film where excellent amorphous stability can be expected. In contrast, T_c almost has no change at around 165°C in the film with Mg concentration from 24.8 to 36.8at%. The results reveal that the $\text{Mg}_{21.5}(\text{Sb}_2\text{Te})_{78.5}$ film exhibits the highest T_c in a wide range of Mg content from 0 to 36.8 at% and higher than GST ($\sim 168^\circ\text{C}$), and thus a better thermal stability and data retention can be expected in the composition.

The temperature for 10-years' data retention was used to evaluate endurance of PCM device. The higher temperature indicates the device can store information for a much longer time. In order to evaluate the data retention of the Mg-doped Sb_2Te films, *in situ* resistance-time (R-t) measurements at an elevated temperature were carried out. The maximum temperature for 10-years' data retention can be extrapolated by fitting the data with the Arrhenius equation¹⁰: $t = \tau \exp(E_a/k_B T)$, where τ is a proportional time constant and E_a is crystallization activation energy. The failure time (t) is defined as the time when the film resistance reaches half of its initial value at a specific isothermal temperature T . The data retention temperature of pure Sb_2Te film for 10-year is only at 40°C , which is in contrast with those at ~ 64 , ~ 93 , ~ 119 and $\sim 121^\circ\text{C}$ with an E_a of ~ 2.37 , ~ 3.03 , ~ 3.35 and $\sim 3.86\text{eV}$, respectively, for $\text{Mg}_{6.1}(\text{Sb}_2\text{Te})_{93.9}$, $\text{Mg}_{9.5}(\text{Sb}_2\text{Te})_{90.5}$, $\text{Mg}_{13.1}(\text{Sb}_2\text{Te})_{86.9}$ and $\text{Mg}_{21.5}(\text{Sb}_2\text{Te})_{78.5}$ films as shown in Fig. 1(c) It indicates that the films with Mg content more than 9.5at% have higher thermal stability compared with the conventional GST film (88.9°C , 2.98eV), and the $\text{Mg}_{21.5}(\text{Sb}_2\text{Te})_{78.5}$ film with the highest T_c exhibits a better data retention.

To investigate crystallization characteristics of Mg-doped Sb_2Te films during phase transformation process, the as-deposited samples were annealed at different temperatures for 3 min in Ar flow and subsequently examined by XRD. Fig. 2 shows the XRD results of the $\text{Mg}_x(\text{Sb}_2\text{Te})_{1-x}$ thin films. No crystallization peak can be observed in the as-deposited $\text{Mg}_x(\text{Sb}_2\text{Te})_{1-x}$ films, as shown in Figs. 2(a) and (c), suggesting an amorphous nature of the films. When Sb_2Te , $\text{Mg}_{6.1}(\text{Sb}_2\text{Te})_{93.9}$, $\text{Mg}_{9.5}(\text{Sb}_2\text{Te})_{90.5}$, $\text{Mg}_{13.1}(\text{Sb}_2\text{Te})_{86.9}$, $\text{Mg}_{21.5}(\text{Sb}_2\text{Te})_{78.5}$ films were annealed at 200°C , clear crystalline peaks appeared in XRD patterns. Each crystallization peak can be indexed according to the PDF card (JCPDS NO. 80-1722), and they were identified to be a hexagonal Sb_2Te phase as shown in Fig 2(b). With increasing Mg content to 21.5at%, the width of the peaks becomes broader, as shown in Fig 2(b), implying that crystalline grains become smaller and Mg atoms in the Sb_2Te serve as a center for the suppression of the amorphous-to-hexagonal phase transition. AFM images as shown in Figs. 2(e) and (f) show that the surface roughness (R_q) of $\text{Mg}_{13.1}(\text{Sb}_2\text{Te})_{86.9}$ and $\text{Mg}_{21.5}(\text{Sb}_2\text{Te})_{78.5}$ films is 1.40 and 1.29nm, respectively. The reduction of R_q indicates that increasing Mg content can improve the surface quality of the films. When Mg content reaches 24.8 at% or more, the films annealed at 200°C exhibit a different crystalline phase that can be ascribed to crystalline Sb (JCPDS NO. 71-1173). The higher content Mg in the film can capture Te atoms forming Mg-Te bonds, leading to the precipitation of the crystalline Sb.

In order to analyze the chemical bonding features, XPS Sb 3d and Te 3d spectra for Sb_2Te , $\text{Mg}_{6.1}(\text{Sb}_2\text{Te})_{93.9}$ and $\text{Mg}_{21.5}(\text{Sb}_2\text{Te})_{78.5}$ films annealed at 200°C were investigated, as shown in Figs. 3(a) and (b), respectively. It is well known that the negative shift of the binding energy increases with the decrease of neighbouring atom electro-negativity from Te(2.1) to Sb(2.05) and Mg(1.31).¹¹ Therefore, Sb 3d and Te 3d binding energy should decrease if part of Sb and Te atoms in Sb-Te bonds are replaced by Mg atoms. Compared Sb 3d and Te 3d binding energy in pure Sb_2Te with those in Mg-doped Sb_2Te films, the peaks shift to lower binding energies with increasing Mg content, indicating that Mg dopants are indeed incorporated into Sb_2Te films, forming the Mg-Sb and Mg-Te bonds. The formation of these bonds can increase total bonding enthalpy and lead to an increase in crystallization temperature and crystallization activation energy,¹²⁻¹³ and thus an enhancement in data retention performance.¹⁴ Beside thermal stability improvement, we can infer that compared with $\text{Mg}_{21.5}(\text{Sb}_2\text{Te})_{78.5}$, the reduced T_c in films with Mg content of 24.8at% or more can be ascribed to that the excessive Mg can bond with Te atoms by broking the Sb-Te bonds and forming the excess weak Mg-Te bonds. This leads to the T_c reduced and precipitation of the crystalline Sb in XRD analysis.

Finally, we used a static tester to record the crystallization time by laser irradiation via tunable laser power and pulse width in the scale of nanoseconds.¹⁵ Fig. 4(a) shows power-time-effect (PET) diagram for $\text{Mg}_{21.5}(\text{Sb}_2\text{Te})_{78.5}$ film. The optical contrast (ΔR) in Fig. 4(a) is defined by the following equation¹⁶: $\Delta R = (R_{\text{after}} - R_{\text{before}}) / R_{\text{before}}$, where R_{before} and R_{after} are the reflectivity before and after irradiation, respectively. Clearly, the diagram can be divided into four regions. With increasing laser power and/or pulse width, the region changes in the order of (I) no change, (II) crystallization, (III) re-amorphization, and (IV) ablation. It is clear that there is no change in reflectivity at lower laser power and/or a short pulse width in the initial region I in Fig. 4(a). As the laser power and/or pulse width increase, the atoms in the film obtain enough energy to overcome the activation barrier, and thus the crystallization behavior occurs, which leads to ΔR increased as shown in region II.

If the laser power and/or pulse width are further increased, re-amorphization of the film appears as shown in region III. Finally, an extremely high laser power and/or long pulse width can decrease ΔR as shown in the IV region, indicating that the film has been ablated.

The relative crystallization (defined as $\Delta R/\Delta R_{\max}^{17-18}$) of the $\text{Mg}_{21.5}(\text{Sb}_2\text{Te})_{78.5}$ film before and after the pump laser-pulse irradiation at various laser power and pulse width is shown in Figs. 4(b)-(e). In Fig. 4(b), the relative crystallization remains almost unchanged at low power of 5mW and starts to increase at the power of 10mW. With further increasing laser power, there is an abrupt increase in the relative crystallization as shown in Fig 4(c), where crystallization time (t_c) are determined to be ~ 250 , ~ 215 , and ~ 195 ns at a laser power of ~ 15 , ~ 20 , and ~ 25 mW, respectively, sufficient for the application in high data recording. Interestingly, the relative crystallization begins to decrease at 225ns at a laser power of ~ 25 mW, indicating that an amorphization process starts. As shown in Fig 4(d)-(e), with increasing laser power from 30mW to 50mW, the t_c are shortened from ~ 125 ns to ~ 52 ns during crystallization process. With a laser power of 50mW, t_c of GST is about 300ns,¹⁹ which is much longer than that of $\text{Mg}_{21.5}(\text{Sb}_2\text{Te})_{78.5}$ film. A complete amorphization process is observed at a lower laser power of 35mW compared with that of GST (70mW) in our previous work.¹⁹ The results confirm that the $\text{Mg}_{21.5}(\text{Sb}_2\text{Te})_{78.5}$ film possesses a fast crystallization speed and a low amorphization power.

To verify the structural stability during repetitive melt-quenching cycles, the optical switching behavior was tested. Fig. 4(f) shows ΔR values for $\text{Mg}_{21.5}(\text{Sb}_2\text{Te})_{78.5}$ film under repeating laser pulses (up to 50) for crystallization and amorphization. The set power of 35mW and pulse width of 200ns, and the reset power of 50mW and pulse width of 100ns were chosen on the basis of the power-time-effect plot. The laser pulses are repeatedly loaded onto the specimen, which simulate cyclic optical switching upon phase transitions. The differences in ΔR between crystallization and amorphization recording are almost constant, suggesting that the film composition is stable under repetitive melt-quenching and crystallization-switching cycles.²⁰

Conclusions

In summary, Mg-doped Sb_2Te films have been investigated systematically in terms of their structural, electrical and optical properties. It is shown that, Mg doping over a wide range from 0 to 21.5at% can increase crystallization temperature and activation energy, leading to improved stability of the amorphous state. The enhanced thermal stability in the Mg- Sb_2Te film comes from the formation of the covalent Mg-Sb bond. The optimal composition is confirmed to be $\text{Mg}_{21.5}(\text{Sb}_2\text{Te})_{78.5}$ with T_c ($\sim 183^\circ\text{C}$), E_a ($\sim 3.86\text{eV}$) and 10yr data retention at $\sim 121^\circ\text{C}$. The crystallization time of $\text{Mg}_{21.5}(\text{Sb}_2\text{Te})_{78.5}$ film is much shorter (52ns) and re-amorphization occurs at a lower laser power (35mW) compared with those of $\text{Ge}_2\text{Sb}_2\text{Te}_5$. $\text{Mg}_{21.5}(\text{Sb}_2\text{Te})_{78.5}$ film with good thermal stability, fast crystallization and low-power amorphization as well as good reversible cyclic ability, would be promising for applications in PCM.

Acknowledgements

This work was financially supported by the National Program on Key Basic Research Project (973 Program) (Grant No. 2012CB722703), the Natural Science Foundation of China (Grant Nos. 61377061, 61306147), the Young Leaders of academic climbing project of the Education Department of Zhejiang Province (Grant No. pd2013092), the Program for Innovative Research Team of Ningbo city (Grant No. 2009B217), and sponsored by K. C. Wong Magna Fund in Ningbo University.

Notes and references

^aFaculty of Information Science and Engineering, Ningbo University, Ningbo 315211, China

^bLaboratory of Infrared Material and Devices, The Advanced Technology Research Institute, Ningbo University, Ningbo 315211, China

^cLaser Physics Centre, Research School of Physics and Engineering, Australian National University; Canberra, ACT 0200, Australia

1 A.V. Kolobov, P. Fons, A.I. Frenkel, A.L. Ankudinov, J. Tominaga, T. Uruga, Nat. Mater. 2004 **3** 703.

2 M.H.R. Lankhorst, B.W.S.M.M. Ketelaars, R.A.M. Wolters, Nat. Mater. 2005 **4** 347.

3 G.X. Wang, Q.H. Nie, X. Shen, R.P. Wang, L.C. Wu, Y.G. Lv, J. Fu, T.F. Xu, S.X. Dai, Mater. Lett. 2012 **87** 135.

4 C. Peng, L. C. Wu, Z.T. Song, F. Rao, M. Zhu, X.L. Li, B. Liu, L.M. Cheng, S.L. Feng, P.X. Yang, J. H. Chu, Appl. Surf. Sci. 2011 **257** 10667.

5 Y.G. Lu, S.N. Song, Z.T. Song, F. Rao, L.C. Wu, M. Zhu, B. Liu, D.N. Yao, Appl. Phys. Lett. 2012 **100** 193114.

6 M. Zhu, L.C. Wu, Z.T. Song, F. Rao, D.L. Cai, C. Peng, X.L. Zhou, K. Ren, S.N. Song, B. Liu, S.L. Feng, Appl. Phys. Lett. 2012 **100** 122101.

- 7 M. Wuttig, N. Yamada, *Nat. Mater.* 2007 **6** 824.
- 8 J. Fu, X. Shen, Q.H. Nie, G.X. Wang, L.C. Wu, S.X. Dai, T.F. Xu, R.P. Wang, *Appl. Surf. Sci.* 2013 **264** 269.
- 9 I. Friedrich, V. Weidenhof, W. Njoroge, P. Franz, M. Wuttig, *J. Appl. Phys.* 2000 **87** 4130.
- 10 F. Rao, Z.T. Song, K. Ren, X.L. Zhou, Y. Cheng, L.C. Wu, B. Liu, *Nanotechnology* 2011 **22** 145702.
- 11 R.P. Wang, D.Y. Choi, A.V. Rode, S.J. Madden, B. Luther-Davies, *J. Appl. Phys.* 2007 **101** 113517.
- 12 S. Raoux, M. Salinga, J.L. Jordan-Sweet, A. Kellock, *J. Appl. Phys.* 2007 **101** 044009.
- 13 M.H.R. Lankhorst, *J. Non-Cryst. Solids* 2002 **297** 210.
- 14 C.C. Chang, C.Y. Hung, K.F. Kao, M.J. Tsai, T.R. Yew, T.S. Chin, *Thin Solid Films*, 2010 **518** 7403.
- 15 J.H. Coombs, A.P. Jongenelis, W.V. Es-Spiekman, B.A. Jacobs, *J. Appl. Phys.* 1995 **78** 4906.
- 16 M.J. Kang, S.Y. Choi, D. Wamwangi, K. Wang, C. Steimer, M. Wuttig, *J. Appl. Phys.* 2005 **98** 014904.
- 17 S. Ziegler, M. Wuttig, *J. Appl. Phys.* 2006 **99** 064907.
- 18 T.J. Park, S.J. Park, D.H. Kim, I.S. Kim, S.K. Kim, S.Y. Choi, *Curr. Appl. Phys.* 2008 **8** 716.
- 19 G.X. Wang, X. Shen, Q.H. Nie, R.P. Wang, L.C. Wu, Y.G. Lu, S.X. Dai, T.F. Xu Y.M. Chen, *Appl. Phys. Lett.* 2013 **103** 031914.
- 20 D. Lee, S.S. Yim, H.K. Lyeo, M.H. Kwon, D. Kang, H.G. Jun, S.W. Nam, K.B. Kim, *Electrochem. Solid-State Lett.* 2010 **13** K8.

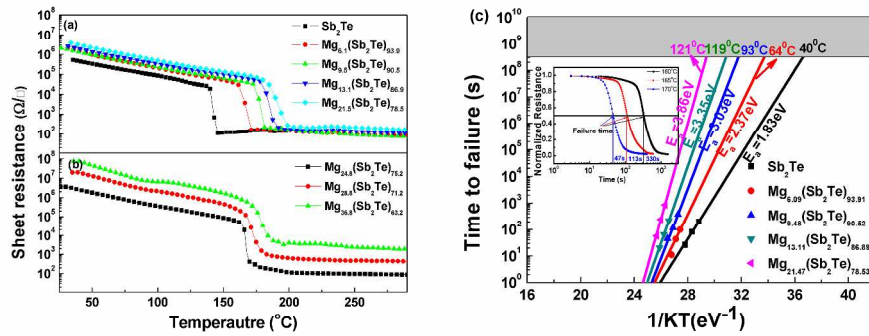


FIG. 1. (a)-(b) Sheet resistance of Mg doped Sb₂Te films as a function of temperature with a heating rate of 40K/min. (c) The extrapolated data retention time of Mg-doped Sb₂Te films at specified temperatures. Inset is the change of resistance with time for the Mg_{21.5}(Sb₂Te)_{78.5} film from measured at certain temperatures.

457x254mm (300 x 300 DPI)

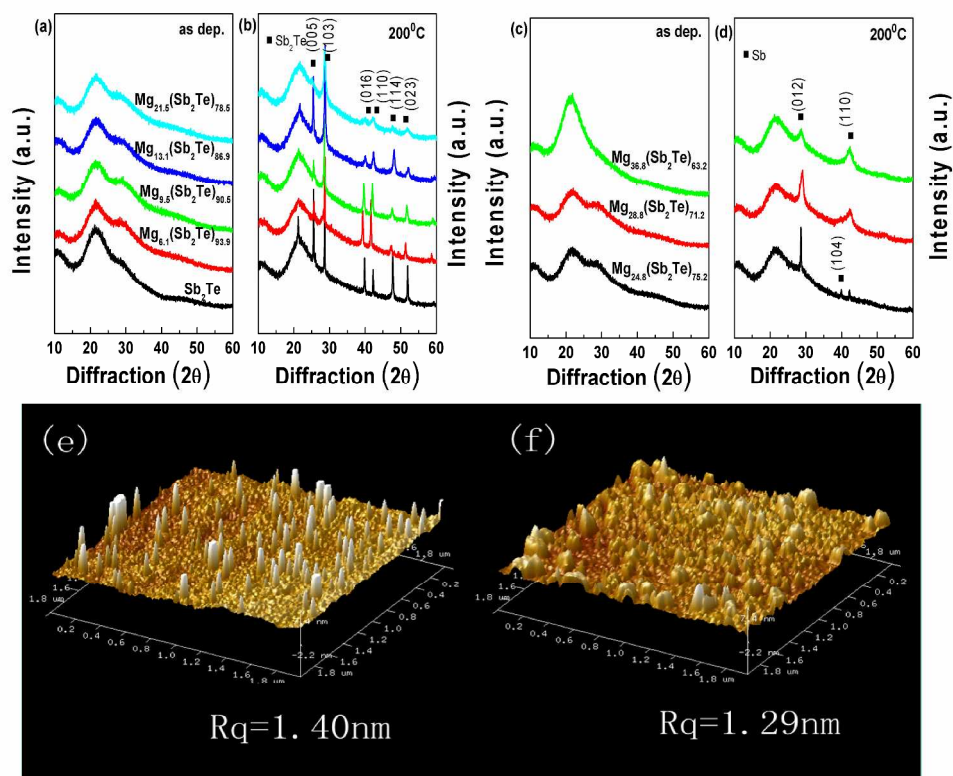


FIG. 2. XRD patterns of Sb₂Te and Mg-doped Sb₂Te films before and after isothermal annealing at various temperatures for 3 min: (a) as-deposited, (b) 200°C, (c) as-deposited, (d) 200°C; The AFM results of the (e) Mg_{13.1}(Sb₂Te)_{86.9}, (f) Mg_{21.5}(Sb₂Te)_{78.5} thin films.

457x457mm (300 x 300 DPI)

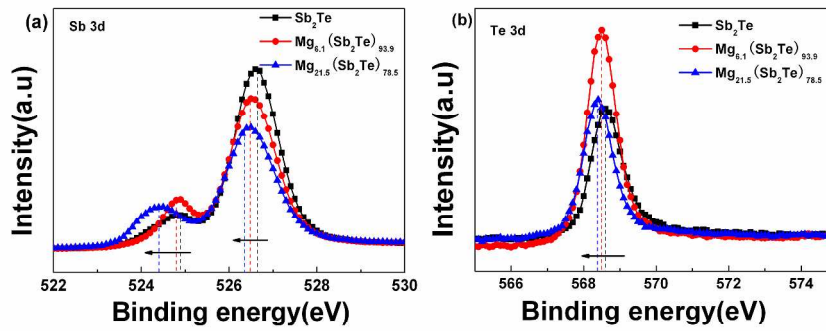


FIG.3 XPS spectra for 200°C-annealed Sb_2Te , $\text{Mg}_{6.1}(\text{Sb}_2\text{Te})_{93.9}$ and $\text{Mg}_{21.5}(\text{Sb}_2\text{Te})_{78.5}$ films: (a) Sb 3d and (b) Te 3d.

458x236mm (300 x 300 DPI)

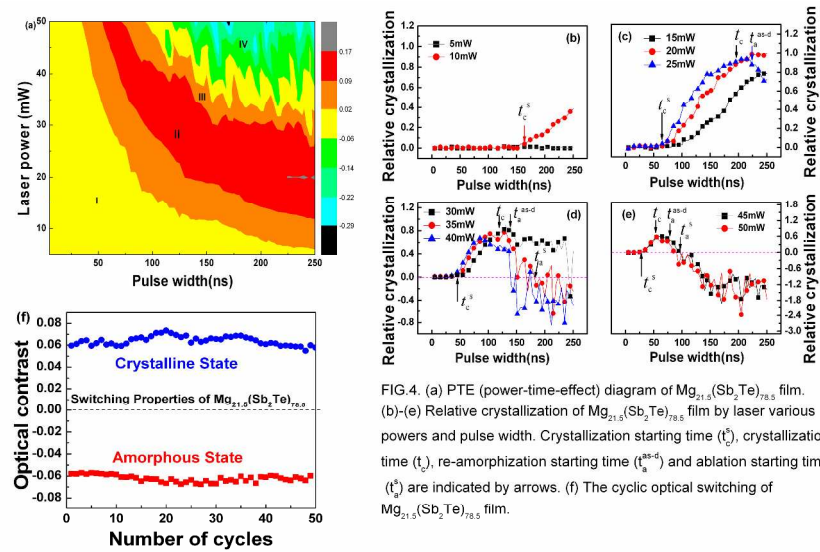


FIG. 4. (a) PTE (power-time-effect) diagram of $\text{Mg}_{21.5}(\text{Sb}_2\text{Te})_{78.5}$ film. (b)-(e) Relative crystallization of $\text{Mg}_{21.5}(\text{Sb}_2\text{Te})_{78.5}$ film by laser various powers and pulse width. Crystallization starting time (t_c^*), crystallization time (t_c), re-amorphization starting time (t_a^{*+}) and ablation starting time (t_a^*) are indicated by arrows. (f) The cyclic optical switching of $\text{Mg}_{21.5}(\text{Sb}_2\text{Te})_{78.5}$ film.

542x328mm (300 x 300 DPI)